THE JOURNAL OF PHYSICAL CHEMISTRY C

Article

Cite This: J. Phys. Chem. C 2018, 122, 9035−9045

pubs.acs.org/JPCC

Effects of Water on Mica−Ionic Liquid Interfaces

Fei Zhang, Chao Fang, and Rui Qiao*

Department of Mechanical Engineering, Virginia Tech, Blacksburg, Virginia 24061, United States

Supporting Information

ABSTRACT: A growing body of work shows that water can affect the structure and properties of the ionic liquids near solid surfaces, which has rich ramifications in applications of ionic liquids such as lubrication and energy storage. Using molecular dynamics simulations, we investigate how water affects the three-dimensional structure of ionic liquids [BMIM][Tf_2N] near mica surfaces with two different charge densities. We show that water can alter not only the layering of ions near the mica surface but also their lateral and orientation ordering and the aggregation of cations' hydrophobic tails. Water often, but not always, weakens the structuring of interfacial ionic liquids. The multifaceted impact of water on the interfacial structure of ionic liquids can be traced back to the fact that water is both a dielectric solvent and a molecular liquid. Based on the additional observations that the adsorption of water at mica−ionic liquid interfaces is enhanced by ionic liquids and surface charge, we suggest that the structure of ionic liquids near solid surfaces is governed by the three-way coupling between the self-organization of ions, the adsorption of interfacial water, and the electrification of the solid surfaces.

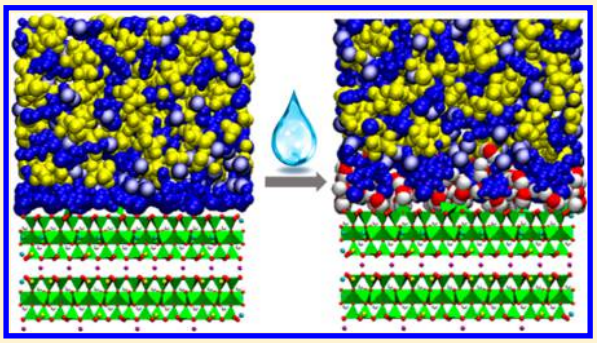

1. INTRODUCTION

Pure room-temperature ionic liquids (RTILs) consist of only ions but remain in the liquid state at temperature below 100 °C.[1,2] Because the molecular structure and combination of the cations and anions in RTILs can be tailored relatively easily and many RTILs offer properties such as wide electrochemical window, low vapor pressure, and excellent thermal stability, RTILs have shown great promise in applications such as capacitive energy storage and lubrication.[3−10] The performance of RTILs in many of these applications depends greatly on the interfacial structures of RTILs near solid surfaces.[1] Therefore, it is essential to gain a fundamental understanding of these interfacial structures.

The interfacial structures of RTILs near solid surfaces have been investigated extensively using experimental,[4,11−18] theoretical,[19−23] and simulation methods.[10,24−36] For example, it is now established that, near charged solid surfaces, cations and anions form alternating layers extending into the RTILs, and the surface charges are often overscreened.[35,37] Interfacial RTILs also exhibit ordering in the lateral directions, thereby making the electrical double layers near charged surfaces three-dimensional (3D) entities. The 3D structure of interfacial RTILs can be modified by factors such as surface charge and confinement.[4,38−42] Few of these studies, however, paid attention to the possible existence of water in RTILs and how the interfacial structures of RTILs are affected by the water. In reality, most RTILs are hygroscopic and can absorb a noticeable amount of water from the environment.[43] Since 2014, these issues have received significant attention.[17,18,22,44−50] For example, using molecular dynamics (MD) simulations, Feng et al. showed that, compared to that in bulk RTILs, water molecules are greatly enriched near electrified graphene surfaces, and the level of enrichment depends on both the surface charge and the choice of RTILs (in particular the counterions near the electrified surfaces).[45] On the experimental front, Gong et al. showed that RTILs form extended layers on a mica surface in ambient environment with a finite relative humidity (hence there is a finite adsorption of water at the RTIL−mica interfaces).[51] Under elevated temperature and when the water on the mica surface is displaced by airborne hydrocarbons, RTILs experience dewetting on the mica surface and form droplets. To explain these observations, they hypothesized that, in the presence of water, mica's surface K^+ ions desorb and exchange with the cations in the RTILs, which triggers the ordered packing of alternating layers of cations and anions near the mica surface and consequently the extended layering of RTILs. Independently, Cheng et al. examined how water affects the interfacial structure of [C_2mim][Tf_2N] liquids near mica surfaces and electrified gold surfaces. Based on surface force measurements, they also suggested that the water molecules adsorbed at the mica−RTIL interfaces profoundly alter the interfacial structure of RTILs by enabling the electrification of the mica surfaces. This idea was further developed in a follow-up study,[18] in which the interfacial structure of RTILs and water was again inferred from the interaction force vs separation curves obtained using atomic force microscopy (AFM) and surface force apparatus (SFA).

Received: February 8, 2018
Revised: March 28, 2018
Published: April 5, 2018

DOI: 10.1021/acs.jpcc.8b01405
J. Phys. Chem. C 2018, 122, 9035−9045

The great impact of water on the interfacial structure of RTILs reported in these studies has been observed in more recent studies,[48,49,52] and it has been further shown that water also significantly modifies other macroscopic observables such as the capacitance of double layers near electrodes.[22] While the importance of water on the interfacial structure of RTILs is generally recognized, a difference in opinion does exist. For example, based on a study of mica−propylammonium nitrate (PAN) interfaces using amplitude-modulated atomic force microscopy, McDonald et al. suggested that the adsorption of water at mica−RTIL interfaces is not essential for the electrification of mica surfaces in contact with some RTILs.[53]

The above experimental and simulation studies triggered many simulation studies of the solid−RTIL interfaces in the presence of water. Among all solids, mica offers an ideal model surface, and the muscovite mica surface is one of the most studied surfaces. Muscovite ($KAl_2Si_3AlO_{10}(OH)_2$) is a phyllosilicate clay with a tetrahedral−octahedral−tetrahedral (TOT) structure. In the muscovite layer, each Al-centered octahedral sheet is sandwiched between two Si-centered tetrahedral sheets, in which every four Si atoms is substituted by Al atoms. The structure thus resulting carries negative charge, which is compensated by the K^+ ions. Neighboring TOT structures are held together by a potassium interlayer and can be cleaved from the (001) plane to form a surface featuring K^+ ions.[54,55]

Previous work suggested that water alters the RTIL structure at mica surfaces.[17,18,51] However, directly visualizing the change of interfacial RTIL structure experimentally is difficult, and the available experimental insight on such a structure change is mostly inferred indirectly from other macroscopic observables such as the force vs distance curves. Such a limitation can be addressed using MD simulations. At present, such simulations are rather limited,[46,50] and only two of them deal with mica surfaces. Fajardo et al.[46] investigated the effect of hydration on the interfacial structure of [BMIM][PF_6] confined in a 1.8 nm gap formed by two charged mica surfaces. They found that water is adsorbed at the interface, and the orientation of $BMIM^+$ ions changes as the water loading in bulk RTIL increases. Zhang et al.[50] studied the effects of different types of RTILs and concentration of water molecules on RTIL−mica interfaces. They found that, with water accumulated at the mica−RTIL interfaces, RTILs are slightly displaced away from the surface. While these studies offered critical insights on how water modifies the structure of mica−RTIL interfaces, they focused mostly on the distribution of ions and water molecules normal to the mica surface, and limited attention has been paid to the 3D structure of *RTILs and water* near open mica surfaces. Understanding the 3D structure of RTILs and how it is affected by the water is important because recent experimental and simulation studies revealed that RTILs can exhibit rich 3D structures near solid surfaces.[1,4,38−42]

In this work, we investigate the interfacial structure of [BMIM][Tf_2N] near mica surfaces using MD simulations. Using atomistic models, we explore the effects of water and surface charging on the 3D structure of RTILs near the mica surfaces. The rest of this manuscript is organized as follows. Section 2 describes the simulation system and methods. Section 3 presents the interfacial structure of [BMIM][Tf_2N] and how it is affected by surface charge and water. Finally, conclusions are drawn in Section 4.

2. SIMULATION SYSTEM, MODELS, AND METHODS

System. We focus on the interfacial structure of RTILs near muscovite mica surfaces in two types of systems. In the first type, a thick film of [BMIM][Tf_2N] is placed on a slab of mica, whose surface is neutral. The system is either free of water (Figure 1a) or features a small amount of water (Figure 1b).

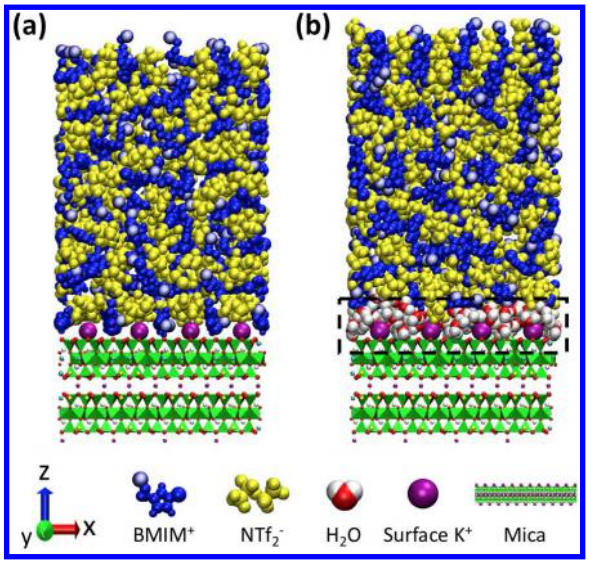

Figure 1. Snapshots of the MD systems for studying the structure of [BMIM][Tf_2N] near neutral mica surfaces in the absence of (a) and in the presence of (b) water in the interfacial zone.

These systems mimic the initial stage of a freshly cleaved mica surface in contact with dry or humid RTILs. Studying these systems can lay a foundation for understanding the electrification of mica surfaces, which involves the dissociation of the surface K^+ ions from mica surfaces.

In the second type of system, a thick film of [BMIM][Tf_2N] is placed on a slab of mica, whose surface K^+ ions are all removed and not included in the MD system. The charge of the mica surface is neutralized by an extra number of $BMIM^+$ ions in the liquid film. These systems mimic the situation in which fully electrified mica surfaces (surface charge density σ is −0.33 C/m^2) are in contact with RTIL baths. Note that in this situation the charge of a mica surface is screened by the ions of the RTILs due to their overwhelming abundance compared to the K^+ ions dissociated from the mica's surface. Same as the first type of system, this second type of system can be either free of water or contain a small amount of water.

All simulation systems measure 3.15 × 3.67 nm^2 in the plane of the mica surface (*xy*-directions) and 15 nm in the direction normal to the mica surface (*z*-direction). In systems with neutral mica surfaces and dry RTIL, 115 pairs of [BMIM]-[Tf_2N] ions are placed on the mica slab, resulting in an ∼6 nm thick liquid layer. Such a liquid layer is thick enough that the RTILs in the middle of the film are neutral, and the structure of the RTILs near the mica surface is not affected by the RTIL−vacuum interface. In simulations with a charged mica surface, there are 139 $BMIM^+$ ions and 115 Tf_2N^- ions in the system.

To study the effect of water on the interfacial structure of RTILs, we introduce 160 water molecules into the RTIL−mica interfacial zone (cf. the black box in Figure 1b) for systems with a neutral or charged mica surface. Our simulations show that these water molecules remain in the interfacial zone during

DOI: 10.1021/acs.jpcc.8b01405
J. Phys. Chem. C 2018, 122, 9035−9045

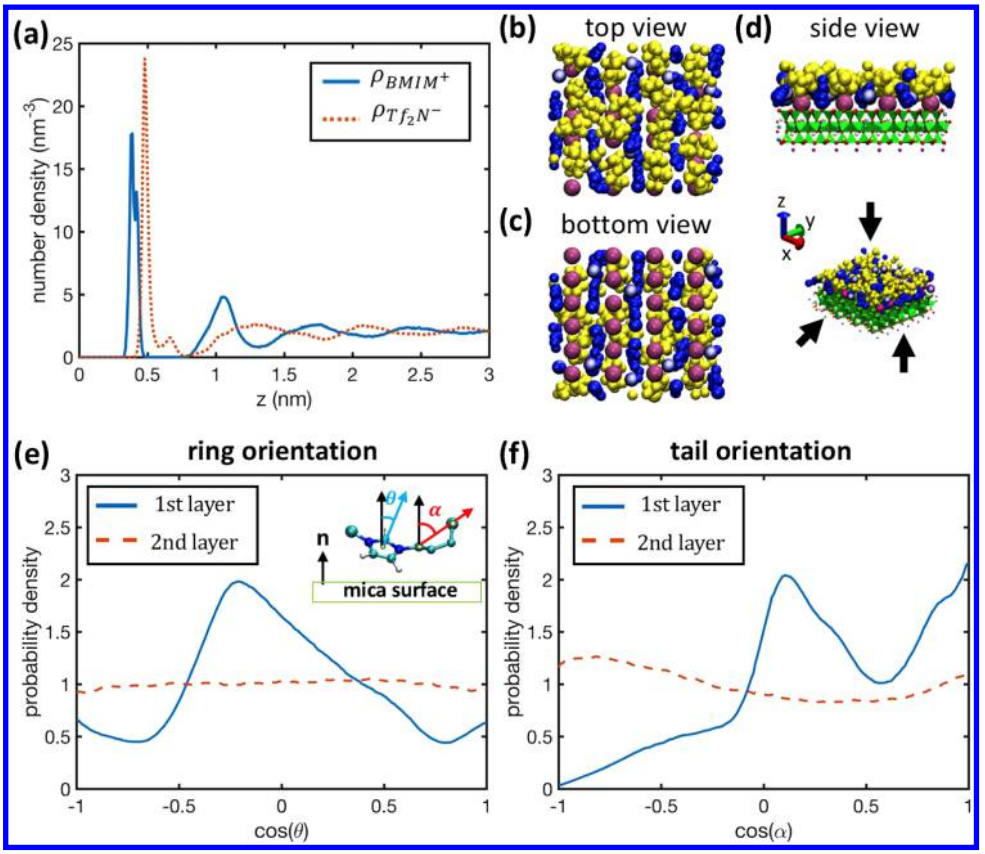

Figure 2. Structure of [BMIM][Tf_2N] liquids near a dry mica surface with a zero net charge density. (a) The density profiles of the cations and anions. The position of the cation (anion) is based on the geometrical center of its ring (its nitrogen atom). (b–d) The top, bottom, and side views of the first layer of cations and anions near the mica surface. The color coding of different species is shown in Figure 1. The last atom on the cation's hydrophobic tail is shown in light blue. (e, f) The probability density distribution of the orientation of the ring (e) and tail (f) of the first and second layer of $BMIM^+$ ions near the mica surface with respect to the normal direction of the mica surface.

production runs of tens of nanoseconds in length. The relative humidity of the virtual ambient environment (T = 300 K) with which the interfacial water is in equilibrium can be computed using (see Supporting Information for derivation)

$$\mathrm{RH} = \frac{k_B T \rho(z_0)}{p_0} \exp\left(\frac{\phi(z_0)}{k_B T}\right) \quad (1)$$

where $\rho(z_0)$ is the water density at a reference point z_0 in the RTIL film. $\phi(z_0)$ is the potential of mean force (PMF) of a water molecule at this point relative to that at a position outside of the RTIL film. k_B is the Boltzmann constant, and p_0 = 3.524 kPa is the saturated vapor pressure of water at 300 K. $\phi(z_0)$ is obtained by computing the PMF of water molecules in *separate* simulations, where water molecules are constrained at a series of positions across the RTIL film, and the Umbrella sampling method is used to extract their PMF (see Supporting Information).

Models. Each mica slab is modeled as two muscovite layers, resulting in a total thickness of ~2 nm. The PCFF force fields are used to describe the mica,[56,57] and water molecules are described using the flexible SPC model.[58] [BMIM][Tf_2N] is modeled using the force fields developed in ref 59. The force field parameters for the nonbonded interactions between RTILs and mica/water are summarized in Table S1.

Simulation Protocol and Method. To build the simulation system, water molecules are placed on the mica surface, and RTILs are packed in the region 1 nm above the mica surface using the Packmol code.[60] An equilibrium run of 10 ns is then performed, during which the RTILs gradually come into contact with the water molecules and mica surface. This is followed by a production run of 40 ns, during which the trajectory is saved every 1 ps.

MD simulations are performed in the NVT ensemble using the LAMMPS code.[61] The temperature of the system is maintained at 300 K using the Nose–Hoover thermostat.[62] A time step of 2 fs is used, and the neighbor list is updated every step. The bonds in the RTILs involving H atoms are constrained using the Shake algorithm. The cutoff for the nonelectrostatic interactions is 1.2 nm. The electrostatic interaction is computed using the PPPM method.[63] While the system is periodic in all directions, the slab correlation has been applied in the calculation of electrostatic interactions to effectively remove the periodicity in the direction normal to the mica surface.

3. RESULTS AND DISCUSSION

3.1. Interfacial Structure near Neutral Mica Surfaces.

We first examine the case where the interfacial zone contains no water. Figure 2a shows the density profiles of ions near the mica surface. The position of the $BMIM^+$ (Tf_2N^-) ion is based on the geometrical center of its imidazole ring (nitrogen atom). The strong peaks at z = 0.39 and 0.48 nm indicate that $BMIM^+$ and Tf_2N^- ions adsorb roughly in a single layer on the mica surface, with the $BMIM^+$ ions slightly closer to the mica. The second density peak of the $BMIM^+$ (Tf_2N^-) ion appears at z =

DOI: 10.1021/acs.jpcc.8b01405
J. Phys. Chem. C 2018, 122, 9035–9045

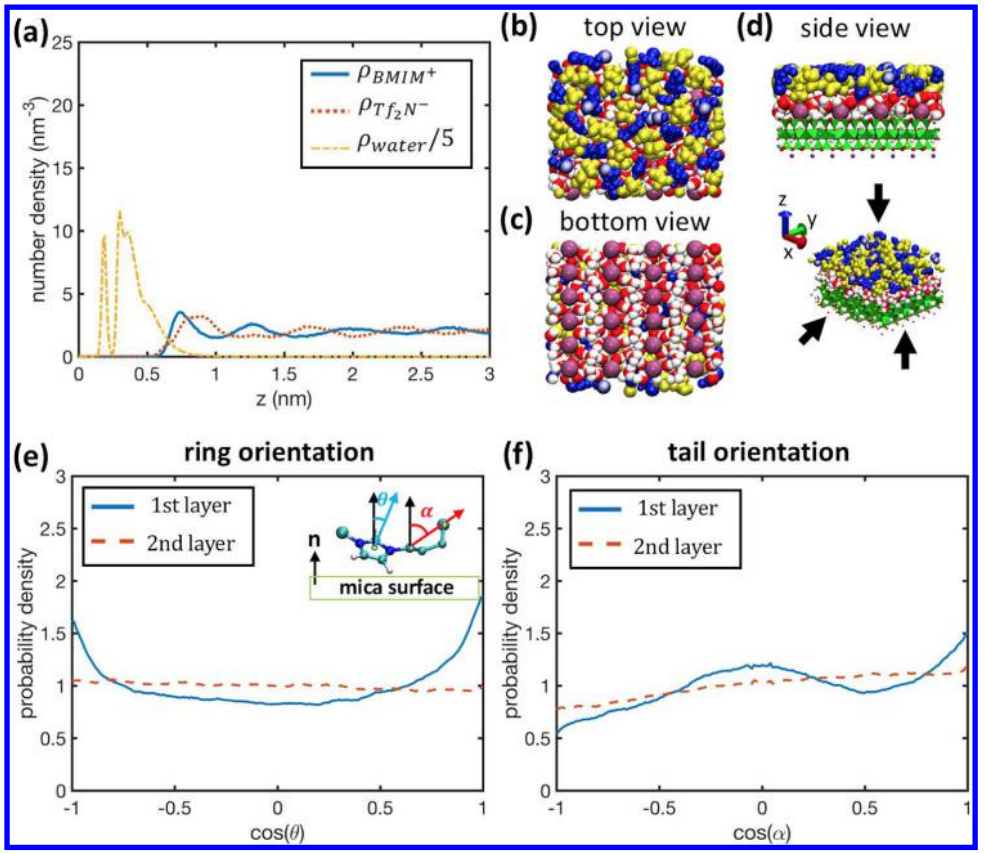

Figure 3. Structure of [BMIM][Tf_2N] liquids and water near a neutral mica surface with a zero net charge density. (a) The density profiles of the cations, anions, and water molecules. The density of water is scaled by a factor of 5, and the position of the water molecules is based on their oxygen atom. (b–d) The top, bottom, and side views of the first layer of cations and anions and all water molecules near the mica surface. (e,f) The probability density distribution of the orientation of the ring (e) and tail (f) of the first and second layer of $BMIM^+$ ions near the mica surface with respect to the normal direction of the mica surface.

1.16 nm (1.31 nm), which is much lower than its first peak. At larger distance from the mica surface, density peaks of both ions diminish. These results suggest that beyond the first ion adsorption layer the layering of both ions is weak.

Since the adsorption of the first cation and anion layers on the mica is strong, we examine the organization of these adsorbed ions. Figure 2b–d shows the top, bottom, and side views of the $BMIM^+$ and Tf_2N^- ions located in their first density peaks. The $BMIM^+$ ions are mostly adsorbed in the interstitial space between the surface K^+ ions, likely due to their affinity to the mica's negatively charged basal oxygen atoms. The Tf_2N^- ions are primarily located above the surface K^+ ions, which explains why the density peak of the Tf_2N^- ions is slightly further away from the mica surface than that of the $BMIM^+$ ions. The adsorbed $BMIM^+$ ions exhibit some orientation ordering. To quantify this ordering, we compute the probability distribution of the orientation of the $BMIM^+$ ions' imidazole rings and butyl tails, i.e., $P(\cos\theta)$ and $P(\cos\alpha)$, where θ (α) is the angle formed by the normal vector of the imidazole ring (the vector pointing from the first to the last carbon atom of the butyl tail) and the normal vector of the mica surface (see Figure 2e,f). These $BMIM^+$ ions' imidazole rings prefer to orient normal to the mica surface (Figure 2e); their tails prefer to lie parallel to the mica's surface or point into the bulk liquids (Figure 2f). Figure 2e,f also shows that, for the $BMIM^+$ ions in the second layer near the mica, their orientation ordering almost vanishes. These results show that, while the interfacial $BMIM^+$ ions exhibit modest structural ordering, this ordering is limited to the adsorption layer. These observations are in line with the study by Cheng et al., in which it was suggested that dry RTILs near freshly cleaved mica exhibit very weak structuring.[17,18]

We next examine the mica–RTIL interface when water is introduced to the interfacial zone. As described above, 160 water molecules are initially placed over the mica surface. Figure 3a shows their density distribution near the mica surface during the last 40 ns of our 50 ns simulation. The water density at $z > 1.0$ nm is nearly zero, indicating that all water molecules remain in the interfacial zone. This is expected: since the load of water in the system far exceeds its solubility in the RTILs, water must be phase separated from the bulk RTILs. Here, water molecules are accommodated on the solid substrate as a thin film because they are stabilized by the hydrophilic mica and, to a less extent, the interfacial RTILs (see below). If the substrate is less hydrophilic, water may phase separate from the bulk RTILs in other forms; e.g., if we remove the partial charge on the mica atoms to make the mica less hydrophilic, the water introduced into the system will form a droplet rather than a thin film on the mica surface (see Figure S4).

The first and second water peaks appear at $z = 0.19$ and 0.30 nm, respectively. The bottom and side views of the interfacial zone indicate that the first peak of water corresponds to the water molecules interacting with the basal oxygen, and the second peak of water corresponds to the water molecules hydrating the surface K^+ ions (see Figure 3c and Figure 3d). Figure 3a also shows that the layer of $BMIM^+$ and Tf_2N^- ions

DOI: 10.1021/acs.jpcc.8b01405
J. Phys. Chem. C 2018, 122, 9035–9045

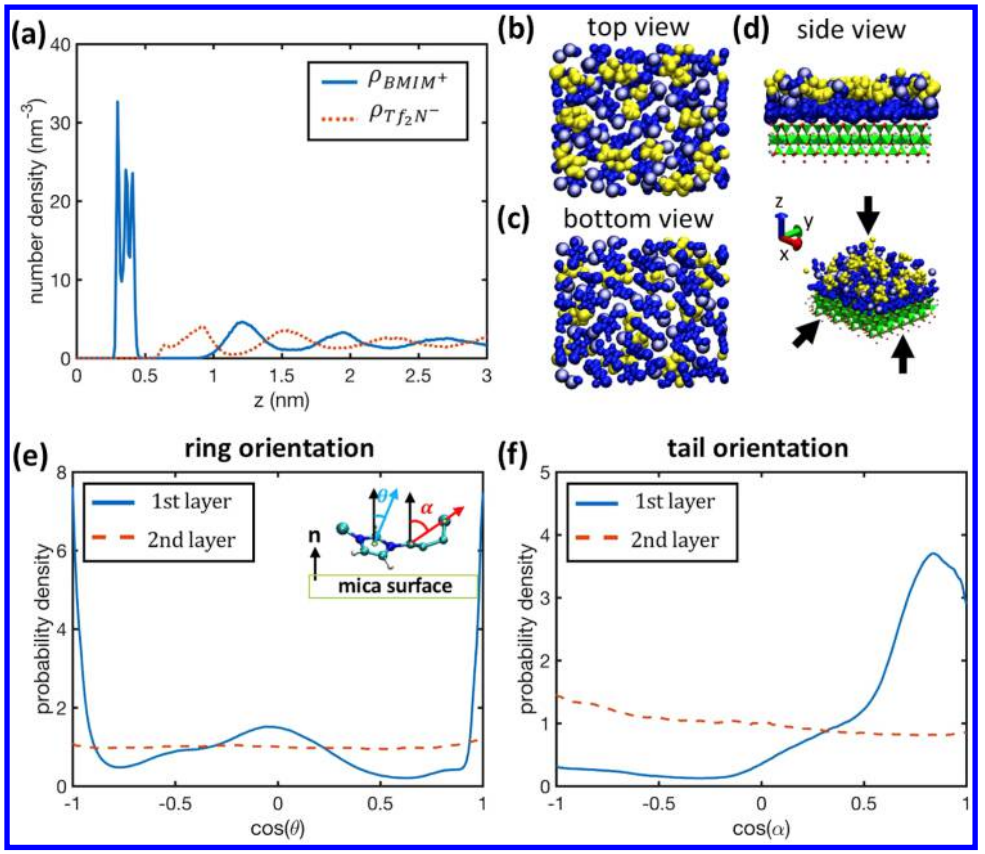

Figure 4. Structure of [BMIM][Tf_2N] liquids near a dry mica surface with a charge density of −0.33 C/m^2. (a) The density profiles of the cations and anions. (b−d) The top, bottom, and side views of the first layer of cations and anions near the mica surface. The color coding of different species is shown in Figure 1. (e,f) The probability density distribution of the orientation of the ring (e) and tail (f) of the first and second layer of $BMIM^+$ ions near the mica surface with respect to the normal direction of the mica surface.

adsorbed on the dry mica surface disappears. Instead, the first peaks of the $BMIM^+$ and Tf_2N^- ions appear at z = 0.75 and 0.88 nm, respectively, and are only modestly higher than the density in bulk liquids. These first peaks are close to each other, suggesting that the charge separation near the mica surface is negligible. The $BMIM^+$ ions in the first density peak exhibit weak orientation ordering, with their rings slightly preferring a coplanar configuration with the mica surface (Figure 3e) and their tails parallel to the mica surface or pointing to the bulk liquids (Figure 3f). The top view of the interfacial zone (Figure 3b) further indicates that the first layer of $BMIM^+$ and Tf_2N^- ions near the mica surface is well mixed, with both ions showing no preferred orientation in the horizontal plane. The comparison of these results with the interfacial structure near dry mica surfaces (see Figure 2) shows that, as water appears at a *neutral* mica−RTIL interface, the layering of RTILs in the z-direction and their lateral structuring are greatly weakened, and the interfacial RTILs appear to be bulk-like.

The above results show that, when water molecules are introduced into the interfacial zone, they outcompete the $BMIM^+$ and Tf_2N^- ions in terms of adsorption on the mica surface. In fact, the water molecules completely displace the $BMIM^+$ and Tf_2N^- ions adsorbed on the mica surface and shifted their density peaks away from the mica surface by ∼0.4 nm. The small size and the dipolar nature of the water molecules are essential for these observations. For a water molecule in the interfacial zone, it shows strong affinity to both the surface K^+ ions (via charge−dipole interactions) and the negatively charged basal oxygen atoms (via hydrogen bonding).[50] The $BMIM^+$ and Tf_2N^- ions, both bulky and carrying delocalized charge, only show affinity to the basal oxygen and surface K^+ ions, respectively. This difference, along with the fact that the ion−mica interactions are screened by the water molecules in the interfacial zone, enables water molecules to displace both ions from the mica surface and become the major molecule solvating the surface K^+ ions. Once water displaces the ionic layers adsorbed on the mica surface, these ions essentially "float" on a molecularly thin film of water. Because the mica surface carries no net charge, neither $BMIM^+$ nor Tf_2N^- ions are attracted to or repelled from it strongly. This, along with the molecular roughness of the thin water film, makes it difficult for these ions to exhibit long-range ordering in both lateral and vertical direction of the mica surface. Consequently, the interfacial ions exhibit much weaker structuring compared to those near dry mica surfaces.

The effects of water on the interfacial structure of RTILs revealed in the above calculations are specific to the water area density at the mica surface adopted here (or equivalently, the relative humidity of the virtual ambient environment, see below). For example, we can expect the first peak of both cations and anions to move closer to the mica surface if a lower water area density is used. Nevertheless, the qualitative aspects of water's effects revealed here should remain; e.g., the weakening of the interfacial structure as water is introduced at the mica−RTIL interfaces.

Using eq 1, the relative humidity of the virtual ambient environment, with which the water molecules of our mica−water−RTIL system are in equilibrium, is found to be 20.5 ±

DOI: 10.1021/acs.jpcc.8b01405
J. Phys. Chem. C 2018, 122, 9035−9045

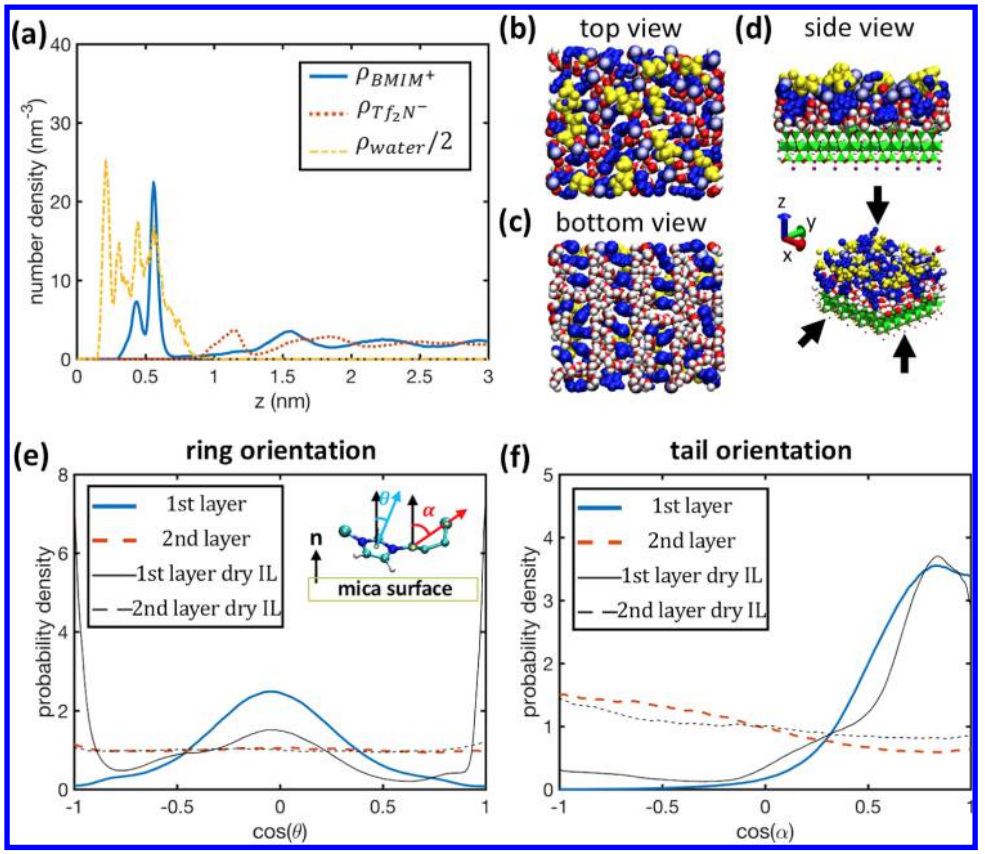

Figure 5. Structure of [BMIM][Tf_2N] liquids and water near a mica surface with a charge density of −0.33 C/m^2. (a) The density profiles of the cations, anions, and water molecules. The density of water is scaled by a factor of 2. (b–d) The top, bottom, and side views of the first layer of cations and anions and all water molecules near the mica surface. (e,f) The probability density distribution of the orientation of the ring (e) and tail (f) of the first and second layer of $BMIM^+$ ions near the mica surface with respect to the normal direction of the mica surface. In (e,f), the orientation distributions of the ring and tail of the $BMIM^+$ ions near dry mica with the same surface charge density are shown for comparison.

11.3% (see Supporting Information). Because nearly all water molecules accumulate near the mica surface, the area density of interfacial water in the present mica–water–RTIL system is 13.8 nm^{-2}. For a bare mica surface exposed to an ambient environment, this area density is obtained when its relative humidity is 76%.[55] Introducing a [BMIM][Tf_2N] film on a mica substrate therefore *enhances* the adsorption of water on its surface. This enhancement is a synergistic effect of two factors. First, water molecules outcompete bulky ions in adsorbing on the mica surface. Second, because the $BMIM^+$ and Tf_2N^- ions near the mica surface can interact with interfacial water molecules via van der Waals and electrostatic forces, these ions provide an energetically more favorable microenvironment for the adsorption of water molecules than the vacuum space above a bare mica surface.

The favorable adsorption of water at mica–RTIL interfaces has practical implications. If not all surface K^+ ions of a mica surface immersed in dry RTILs are dissociated from the mica lattice, then even exposing the RTILs to an environment with low relative humidity will lead to significant adsorption of water on the mica surface. The observation that the surface K^+ ions of mica are readily hydrated by the adsorbed water molecule (Figure 3d) suggests that, similar to the situation of a mica surface immersed in water, surface K^+ ions may dissociate from the mica lattice, thus leaving the mica surface electrified. Hence, we further explore the effect of water on the interfacial structure of RTILs near electrified mica surfaces.

3.2. Interfacial Structure near Charged Mica Surfaces.

We first examine the case where the interfacial zone is free of water. Figure 4a shows the ion density profiles near the mica surface. Three closely positioned peaks, corresponding to a layer of adsorbed $BMIM^+$ ions with different orientations, are observed at z = 0.30, 0.36, and 0.41 nm. This $BMIM^+$ layer is followed by a diffuse Tf_2N^- ion layer centered at z = 0.93 nm. The clear separation of the first $BMIM^+$ and Tf_2N^- ion layers highlights the strong charge separation near the charged mica surface. Alternating layers of $BMIM^+$ and Tf_2N^- ions are observed at larger distance, but the layering of ions is less distinct and becomes rather weak at $z \sim 3.0$ nm. These interfacial structures are consistent with the generic picture of electrical double layers formed by RTILs near electrified surfaces.[1,2,59,64−67]

Beyond ion layering normal to the mica surface, we also examine the lateral and orientation ordering of the interfacial $BMIM^+$ and Tf_2N^- ions. Figure 4b–d shows the top, bottom, and side views of the first layer of $BMIM^+$ and Tf_2N^- ions near the mica surface. $BMIM^+$ ions are seen to displace the Tf_2N^- ions completely from the space adjacent to the mica surface (see Figure 4d). While a distinct lateral ordering of $BMIM^+$ and Tf_2N^- ions is not observed (see Figure 4b and Figure 4c), the $BMIM^+$ ions adsorbed on the mica surface do show preferential orientation. From the distribution of the orientation of the $BMIM^+$ ions' imidazole rings shown in Figure 4e, we observe that their rings prefer to lie parallel to the mica surface ($\cos\theta = \pm 1$) and, to some extent, to align perpendicular to the mica

DOI: 10.1021/acs.jpcc.8b01405
J. Phys. Chem. C 2018, 122, 9035−9045

surface (cos θ = 0, see Figure 4e). From the distribution of the orientation of the $BMIM^+$ ions' tail shown in Figure 4f, we further observe that the adsorbed $BMIM^+$ ions tend to point their tails toward the liquid phase (i.e., away from the mica surface). This preferred orientation is expected because, by staying away from the mica surface, the nearly neutral tails make more room for the charged ring and the methyl group on the ring to accumulate near the highly charged mica surface.[68,69] This observation is also consistent with the prediction by coarse-grained simulations of $[BMIM][PF_6]$ near charged mica surfaces.[46]

We next examine the interfacial structure near mica when water is introduced at the same area density as in the case of neutral mica surfaces. Figure 5a shows the density profiles of water and the ions. Water molecules are again confined within the interfacial zone, and they approach the mica surface closer than the $BMIM^+$ ions. The first layer of $BMIM^+$ ions near the wall, as indicated by the two closely spaced peaks in Figure 5a (z = 0.43 and 0.56 nm), appears at a distance of ~0.5 nm from the mica surface. The position of this $BMIM^+$ ion layer is similar to the position of the $EMIM^+$ layer revealed in the study of humid $[EMIM][BF_4]$ near charged mica surfaces.[50] Compared to the dry mica case (see Figure 4a), the first $BMIM^+$ layer is shifted away from the mica surface by ~0.2 nm, which is similar to that observed in the coarse-grained MD simulations of dry and humid $[BMIM][PF_6]$ confined in a 1.8 nm mica gap.[46] Note that although water molecules appear closer to the mica surface than the $BMIM^+$ ions, whose position is shown using the center of its imidazole ring, the first layer of $BMIM^+$ ions mostly stands on the mica surface with the methyl group on their rings sticking on the surface and their tails up in the liquid. Indeed, as shown in the bottom and side view of the first cation, anion, and water layers near the mica surface (Figure 5c,d), no water molecules get between the first layer of $BMIM^+$ ions and the mica surface. The first $BMIM^+$ layer is followed by a Tf_2N^- layer, whose position is also shifted away from the mica surface by ~0.2 nm compared to the dry mica case. Beyond the first cation and anion layers, alternating layers of $BMIM^+$ and Tf_2N^- ions penetrating to ~3 nm from the mica surface are again observed, although the heights of the corresponding density peaks are lower than the dry mica case.

The above observations are in line with the results from the few simulation studies of RTIL−water−mica interfaces available now.[46,50] Further analysis of the MD trajectories reveals additional insight on how water modifies the structure of RTILs near charged mica surfaces, in terms of ion layering, lateral and orientation ordering, and self-assembly of cations near the mica surface.

We first examine the ion accumulation in the interfacial zone in more detail. We define an accumulative count of the $BMIM^+$ and Tf_2N^- ions using $\Gamma_{\pm}(z) = \int_0^z \rho_{\pm}(s)ds$ and an accumulative excess of cation using $\Gamma_{ex}(z) = \int_0^z (\rho_+(s) - \rho_-(s))ds$. Γ_{ex} indicates how the charge of a mica surface is screened as we move away from the mica surface: the charge is fully screened when Γ_{ex} reaches σ/e and overscreened when Γ_{ex} exceeds σ/e (σ is mica's surface charge density; e is the electron charge). Figure 6a,b compares $\Gamma_{\pm}(z)$ near the mica surface with and without water. It shows that, in the presence of water, the adsorption of $BMIM^+$ on the mica surface is reduced by ~12%, and the number of anions in the first Tf_2N^- ion layer is reduced by ~27%. As a result, the overscreening of the mica's surface charge by the interfacial ions weakens (see Figure 6c).

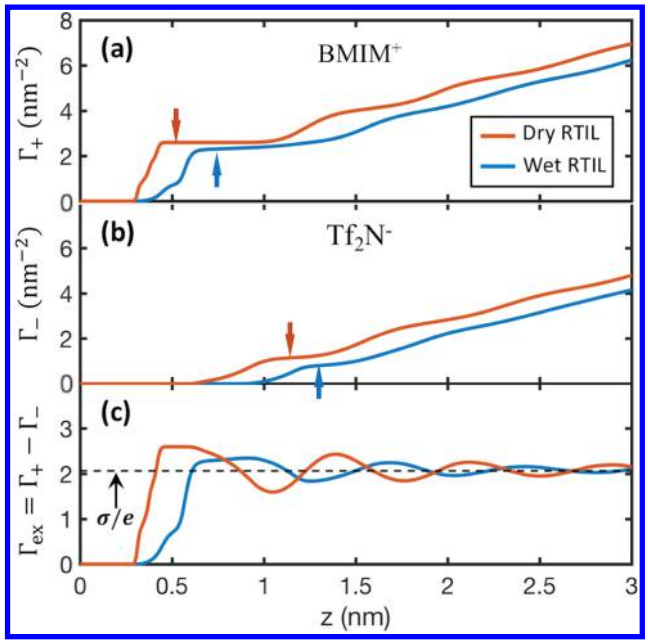

Figure 6. Accumulation of ions near the mica surface with a charge density of −0.33 C/m^2 in the presence and in the absence of water. (a,b) The accumulative count of the $BMIM^+$ ions (a) and Tf_2N^- ions (b) as a function of the distance from the mica surface ($\Gamma_{\pm}(z) = \int_0^z \rho_{\pm}(s)ds$). (c) The accumulative excess of cations as a function of the distance from the mica surface ($\Gamma_{ex}(z) = \int_0^z (\rho_+(s) - \rho_-(s))ds$). In all panels, the outer boundaries of the first $BMIM^+$ and Tf_2N^- layers are marked using arrows.

Along with the reduced $BMIM^+$ adsorption on the mica surface, the ordering of the adsorbed $BMIM^+$ is also modified by the interfacial water. Comparison of Figures 4c and 5c shows that, while the $BMIM^+$ ions adsorbed on dry mica surfaces are largely disordered, those adsorbed on the "wet" mica exhibit strong ordering in the lateral plane. Inspection of the trajectories indicates that these ions are localized at spots where the surface K^+ ions were removed during the electrification of mica surfaces. Figure 5e shows that the $BMIM^+$ ions adsorbed on the mica surface tend to orient their rings normal to the surface, in contrast to the situation near charged, dry mica, where the rings of many of the adsorbed $BMIM^+$ ions lie parallel to the surface. Figure 5f shows that, as in the case of dry mica, the adsorbed $BMIM^+$ ions mostly point their tails toward the bulk liquids. However, compared to that near dry mica, the tails of the second layer of $BMIM^+$ ions near "wet" mica have slightly more preference to orient their tails toward the mica surface. This tail arrangement, along with the fact that the tails of the first layer of adsorbed $BMIM^+$ ions point toward bulk liquids, suggests that the tails of the first two $BMIM^+$ ion layers tend to aggregate. This aggregation, a form of self-assembly often encountered in bulk RTILs,[70] is more distinct near "wet" mica surfaces than near dry mica surfaces.

As with the effect of water on the interfacial structure of RTILs near neutral mica surfaces, the effect of water on the structure of RTILs near charged mica surfaces revealed here is specific to the water area density and mica surface charge density we adopted here. However, the qualitative aspects of water's effect revealed here should persist under other water area densities. In particular, the weakening of overscreening by water is likely a universal phenomenon.

DOI: 10.1021/acs.jpcc.8b01405
J. Phys. Chem. C 2018, 122, 9035−9045

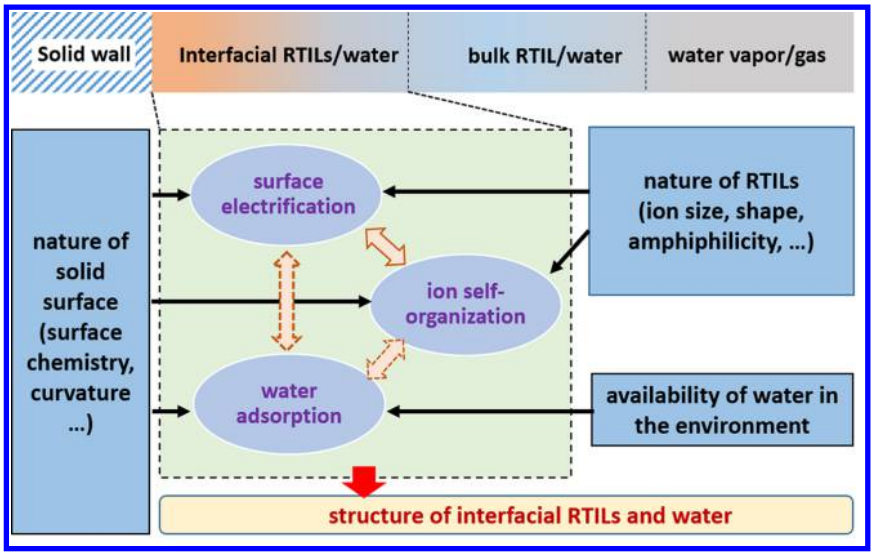

Figure 7. General picture of the structure of room-temperature ionic liquids (RTILs) near solid surfaces that can be electrified by dissociation of the surface atoms. The top panel is a schematic of a solid−RTIL system exposed to the ambient environment. The bottom panel shows the envisioned picture of how the nature of the system (RTILs, solids, and environment) affects the three tightly coupled processes, whose interplay determines the structure of the interfacial RTILs and water.

The multifaceted effects of water on the interfacial structure of RTILs near mica surfaces are caused by the small, but finite, size of water molecules and the dielectric screening by the water molecules. The interactions between a highly charged mica surface and the $BMIM^+$ ions are stronger than that between the mica surface and water molecules. However, once the number of $BMIM^+$ ions adsorbed on the mica surface can fully screen its charge, the smaller water molecule can compete effectively with the bulky $BMIM^+$ ions for the space near the strongly hydrophilic mica surface. In the face of the competition for space by water molecules, the $BMIM^+$ ions must pack more effectively near the mica surface when screening its surface charge. Therefore, $BMIM^+$ ions are adsorbed preferentially on surface spots with more localized negative charge (i.e., the spot below the removed surface K^+ ions), and adsorbed $BMIM^+$ ions align their rings normal to the mica surface. Furthermore, the interfacial water molecules screen the electrostatic interactions between the $BMIM^+$ and Tf_2N^- ions, thus reducing their correlations. Since weaker cation−anion correlations generally reduce the overscreening of surface charge by RTILs,[37] the adsorption of $BMIM^+$ ions on the mica surface and the accumulation of Tf_2N^- ions near the adsorbed $BMIM^+$ ion layer reduce, as observed in Figure 6a and 6b. Because the first Tf_2N^- ion layer near "wet" mica surfaces is less dense compared to that near dry mica surfaces, it leaves more space to accommodate the tails of the ions in the second $BMIM^+$ ion layer near the wall. Therefore, more ions in the second $BMIM^+$ ion layer point their tail toward the mica surface.

While water greatly modifies the structure of interfacial RTILs near charged mica surfaces, the interfacial ions also affect the adsorption of water at the mica−RTIL interface. The area density of interfacial water in the charged mica−water−RTIL system is the same as that in the neutral mica−water−RTIL system. Using eq 1, the relative humidity of the virtual ambient environment, with which the water molecules of our charged mica−water−RTIL system is in equilibrium, is found to be 4.9 ± 3.9% (see Supporting Information), which is lower than that found in the neutral mica system (20.5 ± 11.3%). Therefore, as a mica surface immersed in RTILs develops net charge, the adsorption of water molecules near it is further enhanced.

3.3. General Picture of Ionic Liquid Structure near "Wet" Surfaces. The above results suggest that interfacial water plays three roles in shaping the structure of RTILs near a mica surface. As a dielectric solvent, water screens the electrostatic ion−ion and ion−mica interactions and thus tends to weaken layering at a given surface charge. At the same time, the dielectric screening and hydration of surface atoms by water can prompt the electrification of the mica surfaces, thus enhancing the ion layering near them. As a molecular liquid, water competes with the ions for space near the strongly hydrophilic surfaces, prompts the organization of the hydrophobic tails of the ions, and enforces preferential orientation of the cations' rings, all of which can potentially enhance the ordering of the interfacial ions. The interplay of these roles, which depends on the charge of the mica surface, makes the effect of water on the interfacial ion structure rather complicated. Introducing water can either enhance or weaken the layering of interfacial ions depending on the net charge of the mica surface. Likewise, the lateral and orientation ordering of these ions can be either enhanced or weakened by the introduction of interfacial water.

With the results in the previous sections and prior studies of the interfacial structure of humid RTILs,[17,18,22,44−50] we can postulate a general picture of the structure of RTILs near "wet" surfaces (see Figure 7). Specifically, in the presence of environmental water, the RTIL structure near a surface, whose charge is not dictated by external means (e.g., gold surfaces connected to a voltage source), is governed by *the three-way coupling* among the self-organization of ions, the interfacial water adsorption, and the electrification of the surface. The importance of each process as well as how it depends on input parameters (e.g., nature of RTILs and solid surface and the availability of water in the environment, see the blue boxes in Figure 7) are reasonably established both experimentally and in simulations.[17,18,46,48,50,53] Here, we emphasize that these processes are tightly coupled, and attention should be paid to their interplay in understanding

DOI: 10.1021/acs.jpcc.8b01405
J. Phys. Chem. C 2018, 122, 9035−9045

how input parameters of solid−RTIL−water systems determine the interfacial structure or RTILs. For example, the adsorption of water in the interfacial zone can lead to good hydration of mica's surface K^+ ions, and the self-organization of ions near a mica surface can conceivably modify the local dielectric environment experienced by the surface K^+ ions, both of which can prompt the dissociation of these surface ions and thus the electrification of the mica surface. Furthermore, the adsorption of water at solid−RTIL interfaces is strongly coupled with the ion self-organization and surface electrification. Even some level of positive feedback among the three processes may appear during the development of interfacial structures near an initially uncharged solid surface. As pointed out above, the presence of $[BMIM][Tf_2N]$ on mica surfaces enhances the adsorption of water compared to bare mica surfaces. The adsorbed water may initiate/enhance the electrification of the mica surfaces, which in turn modifies the organization of ions near the surface and attracts even more water molecules to the interfacial zone.

4. CONCLUSIONS

We study the structure of $[BMIM][Tf_2N]$ near mica surfaces with a focus on how the interfacial ion structure is affected by the presence of water and the electrification of mica surfaces. Near dry, neutral mica surfaces, $BMIM^+$ and Tf_2N^- ions, are adsorbed into closely separated layers with little charge separation. The adsorbed $BMIM^+$ ions exhibit modest lateral and orientation ordering, but ions beyond the first layer show very modest structuring. The water molecules introduced at the neutral mica−RTIL interfaces displace the ions from the mica surface, and the structuring of the interfacial ions nearly diminishes. Near dry, highly charged mica surfaces, strong and alternating layering of $BMIM^+$ and Tf_2N^- ions is distinct, but the lateral and orientation ordering of the ions is obvious mainly in the first $BMIM^+$ layer. Introducing water into the system weakens the adsorption of $BMIM^+$ ions on the mica surface and the subsequent layering of Tf_2N^- and $BMIM^+$ ions away from the mica surface. Nevertheless, the lateral and orientation ordering of the $BMIM^+$ ions contact adsorbed on the mica surface becomes stronger, and modest aggregation of the hydrophobic tails of the first and second layers of $BMIM^+$ ions occurs.

Our simulations and insight from prior works on RTIL−water−mica systems suggest a general picture of how water affects the interfacial structure of RTILs; i.e., in the presence of environmental water, the structure of RTILs near a surface electrifiable via surface atom dissociation is governed by *the three-way coupling* between the self-organization of interfacial ions, adsorption of water at RTIL−solid interfaces, and the electrification of the surface. Delineating how these processes and their interplay depend on choice of RTILs, nature of the solid surfaces and the availability of water in the environment will provide a mechanistic understanding of the interfacial structure of humid RTILs near solid surfaces. Research in this direction, especially on the strong coupling of the three processes, can benefit from the integration of different techniques. For example, in this study, the dissociation of the surface K^+ ions is taken as an input because our simulations cannot handle bond breaking. Density functional theory (DFT) simulations capable of resolving the dissociation of surface K^+ ions may be combined with classical MD simulations (or classical DFT simulations) to address this limitation in the future.

Water is often treated as a nuisance in the application of RTILs until most recently. However, at least for water-stable RTILs, water may be leveraged to improve the performance of devices whose function depends on the properties of interfacial RTILs. The concept of tailoring the molecular design of RTILs to obtain desired interfacial structure is widely practiced in applications of RTILs. The idea of using interfacial water as a new handle to manipulate the interfacial structure (and thus dynamics) of RTILs can potentially complement this widely practiced concept and allow more flexibility in the application of RTILs. In this regard, encouraging results have already been reported for using interfacial water to improve capacitive energy storage and lubrication.[8−10] We hope these results will stimulate new fundamental and applied researches on this idea in the future, and the general picture of the interfacial structure of RTILs suggested in this work can help guide these researches.

■ ASSOCIATED CONTENT

Supporting Information

The Supporting Information is available free of charge on the ACS Publications website at DOI: 10.1021/acs.jpcc.8b01405.

Method for computing the relative humidity of the virtual ambient environment with which the interfacial water is in equilibrium and force field parameters (PDF)

■ AUTHOR INFORMATION

Corresponding Author

*E-mail: ruiqiao@vt.edu.

ORCID

Rui Qiao: 0000-0001-5219-5530

Notes

The authors declare no competing financial interest.

■ ACKNOWLEDGMENTS

We thank the ARC at Virginia Tech for generous allocations of computer time and the NSF for support. R.Q. thanks Professor Alexei Kornyshev at Imperial College and Professor Lei Li at University of Pittsburgh for helpful discussions.

■ REFERENCES

(1) Fedorov, M. V.; Kornyshev, A. A. Ionic Liquids at Electrified Interfaces. *Chem. Rev.* **2014**, *114*, 2978−3036.

(2) Hayes, R.; Warr, G. G.; Atkin, R. Structure and Nanostructure in Ionic Liquids. *Chem. Rev.* **2015**, *115*, 6357−6426.

(3) Simon, P.; Gogotsi, Y. Materials for Electrochemical Capacitors. *Nat. Mater.* **2008**, *7*, 845−854.

(4) Perkin, S.; Albrecht, T.; Klein, J. Layering and Shear Properties of an Ionic Liquid, 1-Ethyl-3-Methylimidazolium Ethylsulfate, Confined to Nano-Films between Mica Surfaces. *Phys. Chem. Chem. Phys.* **2010**, *12*, 1243−1247.

(5) Li, H.; Rutland, M. W.; Atkin, R. Ionic Liquid Lubrication: Influence of Ion Structure, Surface Potential and Sliding Velocity. *Phys. Chem. Chem. Phys.* **2013**, *15*, 14616−14623.

(6) Eshetu, G. G.; Armand, M.; Scrosati, B.; Passerini, S. Energy Storage Materials Synthesized from Ionic Liquids. *Angew. Chem., Int. Ed.* **2014**, *53*, 13342−13359.

(7) MacFarlane, D. R.; Tachikawa, N.; Forsyth, M.; Pringle, J. M.; Howlett, P. C.; Elliott, G. D.; Davis, J. H.; Watanabe, M.; Simon, P.; Angell, C. A. Energy Applications of Ionic Liquids. *Energy Environ. Sci.* **2014**, *7*, 232−250.

(8) Fajardo, O. Y.; Bresme, F.; Kornyshev, A. A.; Urbakh, M. Electrotunable Friction with Ionic Liquid Lubricants: How Important

DOI: 10.1021/acs.jpcc.8b01405
J. Phys. Chem. C 2018, 122, 9035−9045

Is the Molecular Structure of the Ions? *J. Phys. Chem. Lett.* **2015**, *6*, 3998−4004.
(9) Lian, C.; Liu, K.; Liu, H. L.; Wu, J. Z. Impurity Effects on Charging Mechanism and Energy Storage of Nanoporous Supercapacitors. *J. Phys. Chem. C* **2017**, *121*, 14066−14072.
(10) Osti, N. C.; Dyatkin, B.; Thompson, M. W.; Tiet, F.; Zhang, P. F.; Dai, S.; Tyagi, M.; Cummings, P. T.; Gogotsi, Y.; Wesolowski, D. J.; et al. Influence of Humidity on Performance and Microscopic Dynamics of an Ionic Liquid in Supercapacitor. *Phys. Rev. Mater.* **2017**, *1*, 035402.
(11) Atkin, R.; Warr, G. G. Structure in Confined Room-Temperature Ionic Liquids. *J. Phys. Chem. C* **2007**, *111*, 5162−5168.
(12) Hayes, R.; Borisenko, N.; Tam, M. K.; Howlett, P. C.; Endres, F.; Atkin, R. Double Layer Structure of Ionic Liquids at the Au(111) Electrode Interface: An Atomic Force Microscopy Investigation. *J. Phys. Chem. C* **2011**, *115*, 6855−6863.
(13) Segura, J. J.; Elbourne, A.; Wanless, E. J.; Warr, G. G.; Voitchovsky, K.; Atkin, R. Adsorbed and near Surface Structure of Ionic Liquids at a Solid Interface. *Phys. Chem. Chem. Phys.* **2013**, *15*, 3320−3328.
(14) Deyko, A.; Cremer, T.; Rietzler, F.; Perkin, S.; Crowhurst, L.; Welton, T.; Steinruck, H. P.; Maier, F. Interfacial Behavior of Thin Ionic Liquid Films on Mica. *J. Phys. Chem. C* **2013**, *117*, 5101−5111.
(15) Griffin, L. R.; Browning, K. L.; Clarke, S. M.; Smith, A. M.; Perkin, S.; Skoda, M. W. A.; Norman, S. E. Direct Measurements of Ionic Liquid Layering at a Single Mica-Liquid Interface and in Nano-Films between Two Mica-Liquid Interfaces. *Phys. Chem. Chem. Phys.* **2017**, *19*, 297−304.
(16) Gebbie, M. A.; Dobbs, H. A.; Valtiner, M.; Israelachvili, J. N. Long-Range Electrostatic Screening in Ionic Liquids. *Proc. Natl. Acad. Sci. U. S. A.* **2015**, *112*, 7432−7437.
(17) Cheng, H. W.; Stock, P.; Moeremans, B.; Baimpos, T.; Banquy, X.; Renner, F. U.; Valtiner, M. Characterizing the Influence of Water on Charging and Layering at Electrified Ionic-Liquid/Solid Interfaces. *Adv. Mater. Interfaces* **2015**, *2*, 1500159.
(18) Cheng, H. W.; Dienemann, J. N.; Stock, P.; Merola, C.; Chen, Y. J.; Valtiner, M. The Effect of Water and Confinement on Self-Assembly of Imidazolium Based Ionic Liquids at Mica Interfaces. *Sci. Rep.* **2016**, *6*, 30058.
(19) Kornyshev, A. A. Double-Layer in Ionic Liquids: Paradigm Change? *J. Phys. Chem. B* **2007**, *111*, 5545−5557.
(20) Liu, L.; Li, S.; Cao, Z.; Peng, Y. X.; Li, G. R.; Yan, T. Y.; Gao, X. P. Well-Ordered Structure at Ionic Liquid/Rutile (110) Interface. *J. Phys. Chem. C* **2007**, *111*, 12161−12164.
(21) Wang, S.; Li, S.; Cao, Z.; Yan, T. Y. Molecular Dynamic Simulations of Ionic Liquids at Graphite Surface. *J. Phys. Chem. C* **2010**, *114*, 990−995.
(22) Friedl, J.; Markovits, I. I. E.; Herpich, M.; Feng, G.; Kornyshev, A. A.; Stimming, U. Interface between an Au(111) Surface and an Ionic Liquid: The Influence of Water on the Double-Layer Capacitance. *ChemElectroChem* **2017**, *4*, 216−220.
(23) Lee, A. A.; Perez-Martinez, C. S.; Smith, A. M.; Perkin, S. Underscreening in Concentrated Electrolytes. *Faraday Discuss.* **2017**, *199*, 239−259.
(24) Shim, Y.; Jung, Y.; Kim, H. J. Graphene-Based Supercapacitors: A Computer Simulation Study. *J. Phys. Chem. C* **2011**, *115*, 23574−23583.
(25) Shim, Y.; Kim, H. J.; Jung, Y. Graphene-Based Supercapacitors in the Parallel-Plate Electrode Configuration: Ionic Liquids Versus Organic Electrolytes. *Faraday Discuss.* **2012**, *154*, 249−263.
(26) Li, S.; Feng, G.; Cummings, P. T. Interfaces of Dicationic Ionic Liquids and Graphene: A Molecular Dynamics Simulation Study. *J. Phys.: Condens. Matter* **2014**, *26*, 284106.
(27) Uysal, A.; Zhou, H.; Feng, G.; Lee, S. S.; Li, S.; Fenter, P.; Cummings, P. T.; Fulvio, P. F.; Dai, S.; McDonough, J. K.; et al. Structural Origins of Potential Dependent Hysteresis at the Electrified Graphene/Ionic Liquid Interface. *J. Phys. Chem. C* **2014**, *118*, 569−574.
(28) Tazi, S.; Salanne, M.; Simon, C.; Turq, P.; Pounds, M.; Madden, P. A. Potential-Induced Ordering Transition of the Adsorbed Layer at the Ionic Liquid/Electrified Metal Interface. *J. Phys. Chem. B* **2010**, *114*, 8453−8459.
(29) Merlet, C.; Rotenberg, B.; Madden, P. A.; Salanne, M. Computer Simulations of Ionic Liquids at Electrochemical Interfaces. *Phys. Chem. Chem. Phys.* **2013**, *15*, 15781−15792.
(30) Merlet, C.; Salanne, M.; Rotenberg, B.; Madden, P. A. Imidazolium Ionic Liquid Interfaces with Vapor and Graphite: Interfacial Tension and Capacitance from Coarse-Grained Molecular Simulations. *J. Phys. Chem. C* **2011**, *115*, 16613−16618.
(31) Fedorov, M. V.; Lynden-Bell, R. M. Probing the Neutral Graphene-Ionic Liquid Interface: Insights from Molecular Dynamics Simulations. *Phys. Chem. Chem. Phys.* **2012**, *14*, 2552−2556.
(32) Feng, G.; Zhang, J. S.; Qiao, R. Microstructure and Capacitance of the Electrical Double Layers at the Interface of Ionic Liquids and Planar Electrodes. *J. Phys. Chem. C* **2009**, *113*, 4549−4559.
(33) Jiang, J.; Cao, D. P.; Jiang, D. E.; Wu, J. Z. Kinetic Charging Inversion in Ionic Liquid Electric Double Layers. *J. Phys. Chem. Lett.* **2014**, *5*, 2195−2200.
(34) Jiang, D. E.; Meng, D.; Wu, J. Z. Density Functional Theory for Differential Capacitance of Planar Electric Double Layers in Ionic Liquids. *Chem. Phys. Lett.* **2011**, *504*, 153−158.
(35) Fedorov, M. V.; Kornyshev, A. A. Ionic Liquid near a Charged Wall: Structure and Capacitance of Electrical Double Layer. *J. Phys. Chem. B* **2008**, *112*, 11868−11872.
(36) Wu, J. Z.; Jiang, T.; Jiang, D. E.; Jin, Z. H.; Henderson, D. A Classical Density Functional Theory for Interfacial Layering of Ionic Liquids. *Soft Matter* **2011**, *7*, 11222−11231.
(37) Bazant, M. Z.; Storey, B. D.; Kornyshev, A. A. Double Layer in Ionic Liquids: Overscreening Versus Crowding. *Phys. Rev. Lett.* **2011**, *106*, 046102.
(38) Kornyshev, A. A.; Qiao, R. Three-Dimensional Double Layers. *J. Phys. Chem. C* **2014**, *118*, 18285−18290.
(39) Perkin, S.; Crowhurst, L.; Niedermeyer, H.; Welton, T.; Smith, A. M.; Gosvami, N. N. Self-Assembly in the Electrical Double Layer of Ionic Liquids. *Chem. Commun.* **2011**, *47*, 6572−6574.
(40) Merlet, C.; Limmer, D. T.; Salanne, M.; van Roij, R.; Madden, P. A.; Chandler, D.; Rotenberg, B. The Electric Double Layer Has a Life of Its Own. *J. Phys. Chem. C* **2014**, *118*, 18291−18298.
(41) Ivaništšev, V.; Fedorov, M. V. Interfaces between Charged Surfaces and Ionic Liquids: Insights from Molecular Simulations. *Electrochem. Soc. Interface* **2014**, *23*, 65−69.
(42) Kirchner, K.; Kirchner, T.; Ivanistsev, V.; Fedorov, M. V. Electrical Double Layer in Ionic Liquids: Structural Transitions from Multilayer to Monolayer Structure at the Interface. *Electrochim. Acta* **2013**, *110*, 762−771.
(43) Wasserscheid, P.; Welton, T. *Ionic Liquids in Synthesis*; Wiley Online Library: New York, 2003.
(44) Yu, Z.; Wu, H. Y.; Qiao, R. Electrical Double Layers near Charged Nanorods in Mixture Electrolytes. *J. Phys. Chem. C* **2017**, *121*, 9454−9461.
(45) Feng, G.; Jiang, X. K.; Qiao, R.; Kornyshev, A. A. Water in Ionic Liquids at Electrified Interfaces: The Anatomy of Electrosorption. *ACS Nano* **2014**, *8*, 11685−11694.
(46) Fajardo, O. Y.; Bresme, F.; Kornyshev, A. A.; Urbakh, M. Water in Ionic Liquid Lubricants: Friend and Foe. *ACS Nano* **2017**, *11*, 6825−6831.
(47) Docampo-Alvarez, B.; Gomez-Gonzalez, V.; Montes-Campos, H.; Otero-Mato, J. M.; Mendez-Morales, T.; Cabeza, O.; Gallego, L. J.; Lynden-Bell, R. M.; Ivanistsev, V. B.; Fedorov, M. V.; et al. Molecular Dynamics Simulation of the Behaviour of Water in Nano-Confined Ionic Liquid-Water Mixtures. *J. Phys.: Condens. Matter* **2016**, *28*, 464001.
(48) Cui, T.; Lahiri, A.; Carstens, T.; Borisenko, N.; Pulletikurthi, G.; Kuhl, C.; Endres, F. Influence of Water on the Electrified Ionic Liquid/Solid Interface: A Direct Observation of the Transition from a Multilayered Structure to a Double-Layer Structure. *J. Phys. Chem. C* **2016**, *120*, 9341−9349.

DOI: 10.1021/acs.jpcc.8b01405
J. Phys. Chem. C 2018, 122, 9035−9045

(49) Zhong, Y. X.; Yan, J. W.; Li, M. G.; Chen, L.; Mao, B. W. The Electric Double Layer in an Ionic Liquid Incorporated with Water Molecules: Atomic Force Microscopy Force Curve Study. *ChemElectroChem* **2016**, *3*, 2221−2226.
(50) Zhang, H.; Zhu, M.; Zhao, W.; Li, S.; Feng, G. Molecular Dynamics Study of Room Temperature Ionic Liquids with Water at Mica Surface. *Green Energy Environ.* **2017**, DOI: 10.1016/j.gee.2017.11.002.
(51) Gong, X.; Kozbial, A.; Li, L. What Causes Extended Layering of Ionic Liquids on the Mica Surface? *Chem. Sci.* **2015**, *6*, 3478−3482.
(52) Anaredy, R. S.; Lucio, A. J.; Shaw, S. K. Adventitious Water Sorption in a Hydrophilic and a Hydrophobic Ionic Liquid: Analysis and Implications. *Acs Omega* **2016**, *1*, 407−416.
(53) McDonald, S.; Elbourne, A.; Warr, G. G.; Atkin, R. Metal Ion Adsorption at the Ionic Liquid-Mica Interface. *Nanoscale* **2016**, *8*, 906−914.
(54) Ho, T. A. *Nanoscale Fluid Transport: From Molecular Signatures to Applications*; Springer: Berlin, Germany, 2017.
(55) Malani, A.; Ayappa, K. G. Adsorption Isotherms of Water on Mica: Redistribution and Film Growth. *J. Phys. Chem. B* **2009**, *113*, 1058−1067.
(56) Heinz, H.; Koerner, H.; Anderson, K. L.; Vaia, R. A.; Farmer, B. L. Force Field for Mica-Type Silicates and Dynamics of Octadecylammonium Chains Grafted to Montmorillonite. *Chem. Mater.* **2005**, *17*, 5658−5669.
(57) Heinz, H.; Suter, U. W. Atomic Charges for Classical Simulations of Polar Systems. *J. Phys. Chem. B* **2004**, *108*, 18341−18352.
(58) Xu, Y.; Liu, Y. L.; Gao, S.; Jiang, Z. W.; Su, D.; Liu, G. S. Monolayer Adsorption of Dodecylamine Surfactants at the Mica/Water Interface. *Chem. Eng. Sci.* **2014**, *114*, 58−69.
(59) Vatamanu, J.; Borodin, O.; Bedrov, D.; Smith, G. D. Molecular Dynamics Simulation Study of the Interfacial Structure and Differential Capacitance of Alkylimidazolium Bis(Trifluoromethanesulfonyl)Imide [$C_n$mim][TFSI] Ionic Liquids at Graphite Electrodes. *J. Phys. Chem. C* **2012**, *116*, 7940−7951.
(60) Martinez, L.; Andrade, R.; Birgin, E. G.; Martinez, J. M. Packmol: A Package for Building Initial Configurations for Molecular Dynamics Simulations. *J. Comput. Chem.* **2009**, *30*, 2157−2164.
(61) Plimpton, S. Fast Parallel Algorithms for Short-Range Molecular-Dynamics. *J. Comput. Phys.* **1995**, *117*, 1−19.
(62) Evans, D. J.; Holian, B. L. The Nose-Hoover Thermostat. *J. Chem. Phys.* **1985**, *83*, 4069−4074.
(63) Hockney, R. W.; Eastwood, J. W. *Computer Simulation Using Particles*; Taylor & Francis Group: New York, 1988.
(64) Li, H.; Endres, F.; Atkin, R. Effect of Alkyl Chain Length and Anion Species on the Interfacial Nanostructure of Ionic Liquids at the Au(111)-Ionic Liquid Interface as a Function of Potential. *Phys. Chem. Chem. Phys.* **2013**, *15*, 14624−14633.
(65) Black, J. M.; Walters, D.; Labuda, A.; Feng, G.; Hillesheim, P. C.; Dai, S.; Cummings, P. T.; Kalinin, S. V.; Proksch, R.; Balke, N. Bias-Dependent Molecular-Level Structure of Electrical Double Layer in Ionic Liquid on Graphite. *Nano Lett.* **2013**, *13*, 5954−5960.
(66) Perkin, S. Ionic Liquids in Confined Geometries. *Phys. Chem. Chem. Phys.* **2012**, *14*, 5052−5062.
(67) Mezger, M.; Schroder, H.; Reichert, H.; Schramm, S.; Okasinski, J. S.; Schoder, S.; Honkimaki, V.; Deutsch, M.; Ocko, B. M.; Ralston, J.; et al. Molecular Layering of Fluorinated Ionic Liquids at a Charged Sapphire (0001). *Science* **2008**, *322*, 424−428.
(68) Fedorov, M. V.; Georgi, N.; Kornyshev, A. A. Double Layer in Ionic Liquids: The Nature of the Camel Shape of Capacitance. *Electrochem. Commun.* **2010**, *12*, 296−299.
(69) Georgi, N.; Kornyshev, A. A.; Fedorov, M. V. The Anatomy of the Double Layer and Capacitance in Ionic Liquids with Anisotropic Ions Electrostriction Vs Lattice Saturation. *J. Electroanal. Chem.* **2010**, *649*, 261−267.
(70) Wang, Y.; Jiang, W.; Yan, T.; Voth, G. A. Understanding Ionic Liquids through Atomistic and Coarse-Grained Molecular Dynamics Simulations. *Acc. Chem. Res.* **2007**, *40*, 1193−1199.

DOI: 10.1021/acs.jpcc.8b01405
J. Phys. Chem. C 2018, 122, 9035−9045